A Single Species, Different Repeatomes: Genomic Plasticity in Passiflora Foetida L.

Arthur Monteiro
Federal University of Pernambuco
Mariela A. Sader
National University of Córdoba
Jéssica Nascimento
State University of Bahia
Gustavo Luna
Federal University of Pernambuco
Daniela Cristina Imig
Herrero College
Andrea Pedrosa-Harand
andrea.harand@ufpe.br
Federal University of Pernambuco

Research Article

Keywords: Centromere, Comparative genomics, Intraspecific variation, Retrotransposons, Satellite DNA

Posted Date: February 26th, 2026

DOI: https://doi.org/10.21203/rs.3.rs-8912911/v1

Additional Declarations: No competing interests reported.

Version of Record: A version of this preprint was published at Chromosome Research on August 3rd, 2026. See the published version at https://doi.org/10.1007/s10577-026-09804-7.

Abstract

The genus *Passiflora* L. comprises approximately 650 species, and exhibits high diversity in the Neotropics, especially the subgenus *Passiflora*. Several species of this subgenus have an abundant repetitive fraction, consistent with their increased genome sizes. However, the repetitive DNA fraction of *Passiflora foetida* (*n* = 10), sister to the other species of the subgenus (*n* = 9) and the species with the smallest genome, has not yet been described in detail. In addition, this species comprises a complex of morphological varieties with a wide geographical distribution. The aim of this study was to characterize the repetitive DNA fraction of *P. foetida*, comparing different accessions of its varieties with the other species in section *Dysosmia* and other sections in the same subgenus. The results showed that *P. foetida* has a proportion of repetitive DNA fraction in part consistent with its small genome size, but with marked intraspecific variation. The LTR Ty1/copia retrotransposons were the most abundant, as in the other species of the subgenus, but Ty3/gypsy represented a much smaller fraction compared to the others. The variation observed within *P. foetida* was greater than that detected among *Dysosmia* species. Satellite DNAs were partly unique and partly similar to species from different subgenera, supporting its phylogenetic position. In addition, one *Dysosmia*-specific satellite showed a proximal chromosomal location, making it the first candidate of a centromeric repeat for the genus, despite its variation in abundance among chromosomes.

1. INTRODUCTION

Angiosperms display extensive genomic variation, encompassing differences in DNA content, chromosome number, and both structural and compositional features of their genome (Jiao et al., 2011; Carta et al., 2020; Carta et al., 2022). Such variation can influence plant evolution in several ways, potentially affecting cell cycle duration, recombination rates, reproductive isolation, and speciation. It may also facilitate the origin of new genes through the insertion and diversification of repetitive elements (Bennett & Leitch, 2005; Jiao et al., 2011; Contreras et al., 2015; Bourque et al., 2018). Nevertheless, the impact of chromosomal changes on the evolution of specific plant lineages is still poorly known.

Plant genomes are composed of both unique and repetitive sequences, with repetitive DNA comprising a substantial proportion of most plant genomes (Heslop-Harrison & Schwarzacher, 2011). Unique or low-copy-number sequences include the majority of protein-coding genes. In contrast, the repetitive fraction is mainly composed of transposable elements and tandemly repeated sequences, such as satellite DNAs and ribosomal DNA (rDNA). Ribosomal DNA encodes ribosomal RNA (rRNA) and therefore plays a central role in ribosome biogenesis (Richard et al., 2008). Both unique and repetitive sequences are valuable for karyotype characterization and comparative cytogenetics analysis, making them essential components to investigate chromosome structure and evolution (Jiang et al., 2019).

The genus *Passiflora* L. includes over 650 species (MacDougal & Tillet, 2022; Kuethe et al., 2024), predominantly distributed throughout the Neotropics, with additional occurrences in other regions of the Americas, Africa, and Asia. It represents the largest genus within the family Passifloraceae Juss. ex Roussel (Cervi & Imig, 2013; Powo, 2025), and is currently divided into six main subgenera: *Astrophea* (DC.) Mast., *Decaloba* (DC.) Rchb., *Deidamioides* (Harms) Killip, *Passiflora* Feuillet & MacDougal (Feuillet & MacDougal, 2003), *Tetrapathea* (DC.) P. S. Green, and *Tryphostemmatoides* (Harms) Killip (Ulmer & MacDougal, 2004; Krosnick et al., 2009; 2013; Buitrago et al., 2018; MacDougal & Tillet, 2022).

The subgenus *Passiflora* comprises approximately 250 species and is primarily characterized by large flowers bearing multiple series of corona filaments. It is the most diverse subgenus in South America and the most widely recognized, largely due to the economic importance of cultivated species such as sour passion fruit (*Passiflora edulis* Sims) and sweet passion fruit (*Passiflora alata* Curtis) (Ulmer & MacDougal, 2004). From a cytogenetic perspective, the subgenus *Passiflora* is characterized by a basic chromosome number of *x* = 9 (Hansen et al., 2006; Sader et al., 2019), with the notable exception of *Passiflora foetida* L., which presents *n* = 10. Phylogenetic studies place *P. foetida* as the earliest-diverging lineage and sister to all other species in the subgenus (Krosnick et al., 2013; Cauz-Santos et al., 2020). Considering an ancestral chromosome number of *x* = 12 for the genus (Melo & Guerra, 2021), the *n* = 10 karyotype of *P. foetida* may represent an intermediate state in a descending dysploid series leading to *n* = 9.

Genome size in *Passiflora* varies by more than an order of magnitude, with the largest genomes found in the subgenus *Passiflora*, reaching up to 1C = 2.6 Mbp in *P. quadrangularis* L. (Yotoko et al., 2011). In contrast, *P. foetida* possesses the smallest genome reported for the subgenus (1C = 0.448 Mbp) (Yotoko et al., 2011). That study also identified a positive correlation between genome size and flower size, suggesting a potential relationship between genome size and adaptive evolution in the group (Yotoko et al., 2011). Analysis of the repetitive fraction in three species (P. *cincinnata* Mast., *P. organensis* Rose, and *P. quadrangularis*) revealed that two retrotransposons' lineages, Ty1/copia/Angela and Ty3/gypsy/Tekay, are the primary contributors to genome size expansion in *Passiflora* (Sader et al., 2021). Despite substantial variation in repetitive element composition and organization, no centromeric sequence has yet been identified in the group, even in well-studied species such as *P. edulis*, whose genome has been assembled at chromosome level (Ma et al., 2021; Xia et al., 2021). More recently, the chromosome-level assembly of *P. foetida* revealed a predominance of Ty1/copia elements and a low abundance of Ty3/gypsy (Zou et al., 2023).

Passiflora foetida is a widely distributed climbing vine native to warm regions of the Americas and the Caribbean. However, it has become naturalized and, in some regions, invasive in other parts of the world, including Africa, South Asia, Australia and Hawaii (Hopley et al., 2021,

2026; Zou et al., 2023). The species exhibits marked floral and vegetative morphological variation with flower colours ranging from purplish to white, which complicates classifications due to extensive character overlap (Svoboda, 2023). This variability has resulted in the application of multiple names to infraspecific taxa (Killip, 1938; Vanderplank, 2013; Svoboda, 2016). Following Vanderplank (2013), six varieties are currently recognized: *P. foetida* var. *foetida* L., var. *nigelliflora* (Hooker), var. *oaxacana* Killip, var. *acapulsensis* Killip, var. *ellisonii* Vanderplank, and var. *baraquiniana* (Lem.) Vanderplank (Vanderplank, 2013). Despite this phenotypic diversity and plasticity, the relationships among these varieties remain poorly resolved.

The aim of this study was to investigate the composition and organization of the repetitive fraction in the genome of different varieties of *P. foetida* (*n* = 10), thereby contributing to a better understanding of the evolutionary mechanisms shaping the repeatome in *Passiflora* and its role in genomic diversity. The usefulness of repeat composition for resolving phylogenetic relationships at intraspecific level and thus for contributing to elucidate species complexes was also addressed. Specifically, we addressed the following questions: (i) What does the repetitive fraction of *P. foetida* reveal about repeatome evolution within the subgenus *Passiflora*? (ii) Is there intraspecific variation in the repeatomes of *P. foetida*? (iii) Which repetitive elements are associated with potential genomic differentiation among the species' varieties? (iv) Are there specific patterns in the organization of the repetitive fraction that support the distinction among varieties? (v) Is there intraspecific variation in the chromosomal distribution of the main satellite DNA sequences identified?

2. METHODOLOGY

2.1 Plant Material

Two accessions of *Passiflora foetida* were obtained for cytogenetic analyses through collaboration with *Passiflora* Germplasm Banks at Embrapa Cerrado (Planaltina, Federal District, Brazil and Embrapa Cassava and Tropical Fruits (Cruz das Almas, Bahia, Brazil). Additional two accessions were collected from different states of northeast Brazil (Fig. 1, Table S1). Plants derived from germinated seeds were cultivated in the Experimental Garden of the Laboratory of Cytogenetics and Plant Evolution, Department of Botany, Federal University of Pernambuco (UFPE). Low-coverage Illumina sequence data for herbarium accessions of *P. foetida* were retrieved from the European Nucleotide Archive (ENA; PRJEB43378, Hopley et al., 2021), and genome assembly reads were obtained from the Genome Sequence Archive (GSA; PRJCA020083, Zou et al., 2023). Geographic maps were generated using QGIS 3.34.1.

2.2 Data Processing, Clustering Analysis, and Satellite DNA Characterization

Sequences from selected *P. foetida* accessions (Hopley et al., 2021; Table S2) were chosen to represent repeatome variation observed within the species, based on their taxonomic identification and geographic distribution, and were used for characterization of its repetitive fraction (Fig. 1, Table S2). Taxonomic identifications were established using vouchers associated with each accession, either deposited at the Missouri Botanical Garden (USA) or inferred from the documented occurrence of specific varieties. In total, 15 accessions were selected, comprising three representatives of each identified variety (Fig. 1, Table S2). Sequence data for the individual Pf001, used for genome assembly (PRJCA020083; Zou et al., 2023), were obtained from the Genome Sequence Archive (GSA).

For interspecific comparative analyses, publicly available sequence data were used for *P. caerulea*, *P. coccinea*, *P. edulis*, *P. incarnata*, *P. ligularis*, *P. quadrangularis*, and *P. suberosa* (PRJEB43378, Hopley et al., 2021), as well as for *P. cincinnata* and *P. organensis* (Sader et al., 2021). Comparison among species of the section *Dysosmia* was based on available data for *P. ciliata* and *P. vesicaria* (PRJEB43378, Hopley et al., 2021), as some accessions initially identified as *P. foetida* were later resigned to these species. Because the genome size of *P. ciliata* is unknown, the same number of reads was used for all three species, and genome coverage was calculated only for species with genome sizes estimates available in the literature. Two species from subgenus *Decaloba* were used as outgroups (Figure S1, Table S3).

All sequences were quality-filtered using a cutoff value of Q ≥ 20, requiring at least 90% of bases to meet or exceed this threshold, using the FASTX-Toolkit (Gordon, 2010; http://hannonlab.cshl.edu/fastx_toolkit/) implemented in RepeatExplorer2. Similarity-based clustering was performed using the RepeatExplorer2 pipeline on the ELIXIR-CERIT Galaxy server (https://www.repeatexplorer-elixir.cerit-sc.cz), applying default parameters and selecting 0.1× genome coverage per sample (Novák et al., 2020). For comparative analyses, reads from the accessions were labelled with unique prefixes, sampled at 0.1× genome coverage each, concatenated, and analysed jointly. Final genome coverage, after automatic sampling by RepeatExplorer2 and removal of mitochondrial and plastid reads, was calculated as: coverage = (r × l) / g, where *r* is the number of reads analysed after clustering, *l* is the read length, and *g* is the haploid genome size in base pairs.

For characterization of the repetitive fraction, clusters representing at least 0.01% abundance were automatically annotated and manually curated following the nomenclature proposed by Neumann et al. (2019). A custom database of *Passiflora* satellite DNA sequences (Sader et al., 2021) was included in both individual and comparative analyses. Unclassified clusters were further analysed by similarity searches using BLASTN against the non-redundant protein sequence database in public repositories (https://blast.ncbi.nlm.nih.gov/Blast.cgi). The proportion

of each repetitive sequence was calculated as the number of reads assigned to each cluster relative to the total number of reads in the final dataset, excluding plastid and mitochondrial sequences.

The dataset used for repeatome characterization of all species and *P. foetida* accessions were also analysed using the TAREAN tool implemented in RepeatExplorer2. TAREAN identifies tandemly organized repetitive DNAs and reconstructs putative satellite DNA (satDNA) consensus sequences based on k-mer analysis (Novák et al., 2017). Tandem organization was further assessed using dot-plot analyses with default parameters in Geneious Prime v.7.0.6. Homology among satellite clusters identified across species was assessed following the classification criteria proposed by Ruiz-Ruano et al., (2016), with minor modifications: monomers sharing 50–80% identity across their entire length were considered different families within the same superfamily; those with 80–95% identity was treated as distinct subfamilies within a family; and sequences with ≥ 95% identity were classified as monomeric variants. For this, we used the Needleman–Wunsch global alignment function in Geneious v.7.0.6.

For the *in silico* analysis of the repetitive fraction in the assembled genome, repeat annotation was conducted using the assembly_repeat_annotation_pipeline (https://github.com/kavonrtep/assembly_repeat_annotation_pipeline/releases), following the developer's official protocol (https://github.com/kavonrtep/assembly_repeat_annotation_pipeline?tab=readme-ov-file). This automated Snakemake-based workflow identifies, classifies, and quantifies repetitive sequences in assembled genomes (Kavonrtep, 2025). The pipeline integrates multiple tools, including RepeatModeler2, RepeatMasker, and customized clustering modules, enabling the construction of a comprehensive repeat library and ensuring standardized and reproducible annotation of genome assemblies. All analyses were performed in accordance with the guidelines provided in the official GitHub repository, ensuring consistency across preprocessing, *de novo* repeat identification, and similarity-based classification steps.

For the visualization of the distribution of tandem repeats in the assembled pseudocromosomes (Zou et al., 2023), manually consensus sequences were also mapped against the genome using Geneious (v. 9.1.8). Subsequently, the results were processed with bedtools v.2.31.0 (Linux) to calculate sequence density within successive 1 kbp sliding windows along the pseudocromosomes. The distribution across the assembled chromosomes was plotted using ShinyCircos (Yu et al., 2018).

2.3 Slide Preparation

Root tips from potted plants and germinated seeds grown on Petri dishes were collected and treated with 2 mM 8-hydroxyquinoline (8-HQ) for 4.5 h at 10°C. Samples were then fixed in Carnoy's solution (ethanol:glacial acetic acid, 3:1) for at least 1 h at room temperature and stored at –20°C. For slide preparation, roots were washed twice in distilled water and digested at 37°C in a solution containing 2% cellulase (Onozuka) and 20% pectinase (Sigma) (v/v) for 1 h. Preparations followed a modified air-drying protocol (Ribeiro et al., 2017). Slides were stained with 1 µg/mL 4',6-diamidino-2-phenylindole (DAPI) in a mounting medium (glycerol:McIlvaine buffer pH 7.0, 1:1; v/v) and visualized under a fluorescence microscope to select the best preparations. Selected slides were destained in Carnoy's fixative for 30 minutes and in absolute ethanol for 1 h and then stored at − 20°C until further use.

2.4 Fluorescence *in Situ* Hybridization (FISH)

Fluorescence *in situ* hybridization (FISH) experiments were performed following the protocol described by Pedrosa et al. (2002), using 5S rDNA probes (four oligomers based on conserved angiosperm sequences, pre-labelled at 3' with Cy3 – Pre-Labelled Oligomer Probes, PLOPs - synthesized by Macrogen; Waminal et al., 2018) and 35S rDNA (clone p*Ta*71; Gerlach & Bedbrook, 1979), as well as the satellite DNAs Pqu01-100 and PquSat06-1083 (Sader et al., 2021). Except for the PLOPs, the remaining probes were labelled via nick translation using Cy3-dUTP, and Alexa488-dUTP was used for the p*Ta*71 probe.

Additionally, the most abundant satellite DNA sequence (PfoSat01-27) was synthesized as a pre-labelled oligonucleotide probe (Macrogen) with a Cy3 molecule at the 3' end and hybridized using the non-denaturing FISH (ND-FISH) protocol adapted from Cuadrado et al., (2009). A hybridization solution (30 µL) containing 1 pmol (25 ng) of probe in 2× SSC was applied, slides were covered with plastic coverslips and incubated in a humid chamber at room temperature for 2 hours. After incubation, coverslips were removed and the slides mounted in a DAPI-containing mounting medium (glycerol:McIlvaine buffer, pH 7.0, 1:1; v/v), followed by analysis. FISH images were captured using a Leica DM5500B epifluorescence microscope equipped with a DFC 340FX digital video camara and the AF6000 software (Leica). The best-quality metaphase spreads were selected, captured images for each filter were superimposed using the lighten modus for the signal layers, pseudo coloured using the image adjustment Hue/Saturation function, and uniformly processed for brightness and contrast using Adobe Photoshop® (v.23.1.1).

2.5 Phylogenetic analysis

Plastome sequences from all 15 accessions and species were assembled through reference-based mapping using Geneious v.6.0.3 (Kearse et al., 2012), with the complete plastome of *Passiflora foetida* (NC_043825.1) serving as the reference. Reads were mapped using the default parameters of the "Map to Reference" function, and the resulting consensus sequences were aligned with MAFFT (Katoh & Standley, 2013). For

the intraspecific phylogenetic analyses, six complete plastomes representing species from *Passiflora* genus were included as outgroups: *P. oerstedii* Mast (NC_038124.1), *P. menispermifolia* Kunth (NC_043826.1), *P. retipetala* Mast (NC_038188.1), *P. mucronata* Lam (NC_053312.1), *P. edmundoi* Sacco (NC_053309.1), and *P. watsoniana* Mast (NC_053315.1). For the interspecific plastome phylogenetic analysis, species from section *Decaloba* were included, specifically *P. organensis* Gardner and *P. suberosa* L. In addition to the intraspecific plastome tree, a nuclear topology was also inferred using *P. foetida* rDNA cistron (MH768301.1) as the reference, with *P. organensis* designated as the outgroup.

Interspecific phylogenetic inference was performed using FastTree v.2.1.11 (Price et al., 2009), implemented as a plugin in Geneious v.6.0.3 (Kearse et al., 2012), with default settings. Phylogenetic inference among accessions was conducted within a Bayesian framework using BEAST v.10.5.0 (Suchard et al., 2018). The final alignment contained less than 20% missing data. Two independent Markov chain Monte Carlo (MCMC) analyses were run for 50 million generations each, sampling every 5,000 generations. A GTR substitution model with four gamma-distributed rate categories, a Yule speciation prior, and an uncorrelated relaxed molecular clock were applied (Drummond et al., 2006). After discarding the first 10% of samples as burn-in, convergence and effective sample sizes (ESS) were assessed using Tracer v.1.7.2 (Rambaut et al., 2018). A maximum clade credibility tree was generated with TreeAnnotator (BEAST package), and node support was evaluated using Bayesian posterior probabilities. The calibration point for the plastome dated tree was sourced from TimeTree (Kumar et al., 2017), which references a 32-million-year-old origin for *Passiflora*.

3. RESULTS

3.1 Individual characterization of the repetitive fraction of *P. foetida*

The genome of *P. foetida* was individually characterized using accession PF018, revealing 86 repetitive clusters with an abundance greater than 0.01%, totalling 270,621 reads which corresponded to approximately 47% of the genome (Table 1). The Ty1/copia retrotransposon superfamily was the most abundant, representing 29.01% of the genome, with the Angela lineage alone accounting for 23.24%. The remaining Ty1/copia lineages ranged from 0.06% to 5.45%. Satellite DNA (satDNA) accounted for 4.47% of the genome and was distributed across seven clusters, exceeding the proportion of Ty3/gypsy retrotransposons, which comprised only 3.34%. Within the Ty3/gypsy superfamily, the non-Chromovirus Athila lineage was the most represented (1.92%), followed by Tekay (1.37%) and CRM (0.05%). Unclassified retroelements contributed 5.66% to the genome, whereas other unclassified sequences accounted for approximately 1.72%. Ribosomal DNA sequences were present at lower proportions, with 5S and 35S rDNA representing 0.08% and 2.97% of the genome, respectively.

These values were consistent with those obtained from the complete genome assembly, despite the increase in total repetitive abundance from approximately 47% in the short-read analysis to ~ 62% in the whole-genome assembly. The assembled genome revealed higher abundances for all transposable elements, except for MuDR_Mutator, including approximately 7.39% for the Ty3/gypsy superfamily, although this proportion remained lower than that of Ty1/copia, which reached 40.62%. Tandem repeats, however, were possibly underestimated in the assembly (1.82%). In addition, the genome assembly enabled the detection of additional lineages within both superfamilies, reflecting the broader sampling of repetitive sequences provided by a largely complete, highly continuous genome. Nevertheless, differences might also result from variation present between sequenced accessions (Table 1).

Table 1
Repeatome characterization of *P. foetida* based on individual analyses performed with RepeatExplorer on short reads (accession PF018) or whole genome assembly. Number of sequences automatically sampled for the clustering analysis and resulting coverage for the short read analysis are indicated

	Passiflora foetida	
Sequence source	Short reads	Complete assembly
Reads	293,400	
Coverage	0.1×*	
Repeat		
Class I		
LTRs Ty3/gypsy	3.34%	7.39%
Chromovirus		
CRM	0.05%	0.12%
Galadriel	-	0.22%
Reina	-	0.47%
Tekay	1.49%	4.10%
Non-chromovirus		
Athila	1.31%	2.41%
Ogre	-	-
LTRs Ty1/copia	29.01%	40.62%
Ale	-	0.16%
Alesia	-	0.02%
Angela	23.24%	31.30%
Bianca	0.13%	0.37%
Ikeros	0.06%	0.17%
Ivana	-	0.21%
SIRE	5.45%	7.38%
TAR	-	0.18%
Tork	0.13%	0.80%
Unclassified LTR's	5.66%	4.98%
LINEs	-	7.17%
Pararetrovirus	-	0.05%
Class II		
hAT	-	0.16%
CACTA	-	0.01%
MuDR_Mutator	0.02%	0.01%
PIF_Harbinger	-	0.01%
SatDNA	4.47%	1.82%
rDNA		
*Genome size (1C) = 440,1 Mpb (Yokoto, 2011)		

	Passiflora foetida	
5S	0.08%	-
35S	2.97%	0.41%
Unclassified	1.72%	0.01%
Total	47.29%	62.52%
*Genome size (1C) = 440,1 Mpb (Yokoto, 2011)		

Of the seven clusters identified as tandem repeats, one showed high confidence according to the TAREAN tool implemented in RepeatExplorer2, five showed low confidence, and one was identified based on sequence similarity with the *Passiflora* database (Table 2). Three clusters were shared among species: two (CLs 34 and 75) showed similarity to satDNAs from *P. quadrangularis*, and one (CL 70) to PorSat04-1800 from *P. organensis*. Conversely, four clusters were not detected in the database, two of which (clusters 2 and 28) were similar to each other (85.2% identity) and were therefore considered to belong to the same satDNA family (PfoSat01-27). Consequently, three potentially species-specific satellite DNA families were identified: PfoSat01-27, a minisatellite (3.34% in abundance), PfoSat02-31 (0.31% in abundance), also a short repeat, with partial similarity to 35S rDNA, and PfoSat03-447, the only high-confidence cluster, with a monomer length of 447 bp and an abundance of 0.01%. The remaining clusters displayed abundances ranging from 0.65% to 0.05% in the individual analysis (Table 2; Figure S2).

Table 2

Satellite DNAs identified in *Passiflora foetida* individual analysis, as well as in the comparative analyses within the subgenus *Passiflora*, and within the section *Dysosmia*. Cluster number, monomer size, GC content and TAREAN confidence level are indicated for the individual analysis

	PfoSat01-27	**PfoSat02-31**	**PfoSat03-447**	**PquSat01-100**	**PquSat02-145**	**PquSat06-1083**	**PorSat01-161**	**PorSat04-1800**	**PclSat01-697**
P. foetida individual analysis									
Cluster	2/28	31	107	34	-	75	-	70	-
Monomer size (pb)	27	55	447	1851	-	137	-	2487	-
GC%	50%	77.4%	38.5%	50%	-	37.2%	-	29.7%	-
Confidence of TAREAN	Low	Low	High	Low	-	-	-	-	-
Abundance	3.34%	0.31%	0.01%	0.63%	-	0.05%	-	0.11%	
Comparative analyses									
Subg. Passiflora									
P. caerulea					0.04%				
P. cincinnata									
P. coccinea					0.03%				
P. edulis					0.06%				
P. foetida	3.98%								
P. incarnata					0.01%				
P. liguralis									
P. quadrangularis					0.05%				
Subg. Decaloba									
P. organensis							0.97%		
P. suberosa									
Section Dysosmia									
P. ciliata	2.95%			0.42%				0.01%	0.84%
P. foetida	**1.28%**			**0.36%**		**0.04%**		**0.11%**	
P. versicaria	1.11%			0.21%		0.02%		0.10%	

In silico analysis of the repetitive fraction of the *P. foetida* genome confirmed an enrichment of the Ty1/copia superfamily in proximal chromosomal regions compared to Ty3/gypsy elements, which were less abundant and more dispersed along the chromosomes. Only three of the satellite families identified in the individual analysis of short reads were successfully mapped onto the *P. foetida* pseudomolecule, as well as the 35S rDNA, detected in four chromosome pairs, while the 5S rDNA was present in a single pair (Fig. 2A, S3).

The satellite PfoSat01-27 was detected in nine chromosomal pairs, with prominent peaks on pseudomolecules 1, 3, 7, 8, 9, and 10, whereas smaller or absence of peaks were observed on the remaining chromosomes, particularly pseudomolecule 4. Among the satellites shared with other species, PquSat06-1083, previously described for *P. quadrangularis*, was mainly detected on pseudomolecules 1 and 7, while PorSat04-1800, shared with *P. organensis*, was identified on pseudomolecules 3 and 9, both with monomers of different sizes when compared to the consensus of the other species (Fig. 2B).

The distribution of major repetitive lineages indicated that Ty3/gypsy Athila and Tekay elements were dispersed along the chromosomes but showed a tendency to accumulate along extended proximal chromosomal regions, as observed, for exemple, in LG10. A similar pattern was observed for Ty1/copia SIRE and Angela elements, with Angela being especially abundant in these regions (Fig. 2C).

The most abundant satellites in *P. foetida* were further analysed by *in situ* hybridization (Fig. 3). PfoSat01-27, identified as the most abundant tandem repeat, produced signals on nine chromosomal pairs across the analysed accessions, confirming the *in silico* results and showing a predominant (peri)centromeric localization. These signals were adjacent to, but not co-localized with the 35S rDNA loci, which were detected on three chromosomal pairs, one of them exhibiting weaker signal intensity (Fig. 2, 3a–f). Variation among accessions was observed in the distribution of 5S rDNA, with one accession presenting an additional weak terminal pair of signals (Fig. 3a), whereas the others showed a single pair (Fig. 3c and 3e), consistent with the *in silico* genome analysis (Fig. S3). Heteromorphic chromosomal pairs differing in signal intensity for both 5S rDNA and PfoSat01-27 were also detected (Figs. 3 and 4).

Satellite DNA PquSat01-100 accounted for approximately 0.6% of the repetitive fraction of *P. foetida* and showed proximal blocks that may correspond to 35S rDNA (Fig. 3g). In contrast, PquSat06-1083 exhibited a pericentromeric signal restricted to a single chromosome pair (Fig. 3h).

3.2 Comparative analysis among species of the subgenus Passiflora

A comparative analysis was conducted including previously characterized species of the subgenus *Passiflora*: *P. cincinnata*, *P. edulis*, and *P. quadrangularis* (Sader et al., 2021), as well as species whose repeatome were described here for the first time (*P. caerulea*, *P. coccinea*, *P. incarnata*, and *P. ligularis*). Additionally, two species from the subgenus *Decaloba* were selected as outgroups: *P. organensis* and *P. suberosa* (Table S4).

The comparative characterization of the repetitive genome fraction revealed a total of 199 clusters with an abundance higher than 0.01% across the analysed genomes, with the repetitive fraction ranging from 16.79% to 78.56% (Table S4). Marked variation was observed in the contribution of retroelement superfamilies among species. The Ty1/copia retrotransposon superfamily was the most abundant not only in *P. foetida*, but also in *P. coccinea* and *P. cincinnata*. Within this superfamily, the Angela lineage predominated, representing most of the Ty1/copia fraction (Table S4, Fig. 5, S4).

In contrast, the Ty3/gypsy retrotransposon fraction was more abundant in the remaining species, ranging from 27.28% in *P. incarnata* to 47.81% in *P. ligularis*, including the *Decaloba* outgroup species (11.96% and 31.51%). Tekay was the most abundant lineage within this superfamily, followed by Athila, which was particularly prevalent in *P. caerulea* (12.75%) and *P. edulis* (12.76%). Class II elements were consistently present at low proportions across all analysed species (Table S4, Fig. 5, S4). Tandem repeat sequences exhibited substantial variation among species. The 35S rDNA was most abundant in *P. foetida*, whereas *P. quadrangularis* exhibited the lowest proportion (0.8%). Although generally present at low levels, 5S rDNA reached its highest abundant in *P. incarnata* (0.24%). Satellite DNA sequences were present at low abundances, below 1%, in most species, except for *P. foetida*. No satellite DNA was detected in *P. cincinnata*, *P. ligularis* or *P. suberosa* (Table S4).

Figura 5. Comparative analysis of repetitive DNA in *Passiflora* genomes of the subgenera *Passiflora* and *Decaloba* (outgroup) represented according to their phylogenetic relationships inferred from plastome assemblies using *P. edulis* as reference. **a.** Abundances per repeat class and lineage as percentage of the total genome size; **b.** Abundances per cluster proportional to the sizes of the bars. Annotations indicated by colours.

The comparative analysis recovered four clusters showing similarity to satDNA present in the database. PquSat02-145 and PorSat01-161 were identified as high-confidence satellites, while the satellite PfoSat01-27 appeared in two clusters and was classified as a low-confidence satellite. PquSat02-145 was the most widely shared among the analysed species and exhibited low sequence divergence, reaching its highest abundance in *P. edulis* (0.06%) and its lowest in *P. incarnata* (0.01%). Overall, the satellites identified in the comparative analysis exhibited abundances below 1% of the genome. The only exception was satDNA PfoSat01-27, which accounted for 3.98% of the *P. foetida* genome in this comparative analysis and was detected only in this species (Table 2).

3.3 Comparative analysis among accessions and varieties of *P. foetida*

The comparative analysis among different *P. foetida* accessions revealed a wide variation in the composition of the repetitive genome fraction, ranging from 24.58% to 64.10% (Table S5). *Passiflora foetida var. baraquiniana* and *var. foetida* showed considerable variation, with repetitive fractions spanning from 24.58% (Pf008) to 49.42% (Pf018) and from 27.65% in Pf057 to 55.99% in Pf031, respectively. *Passiflora foetida var. ellisonii* was characterized by the highest repetitive fractions, ranging from 52.83% (Pf001) to 64.10% (Pf064) (Fig. 6, S5).

Class I elements were the most representative repetitive components across all accessions. Within the Ty1/copia superfamily, the Angela lineage predominated in all varieties but exhibited marked variation in abundance, with the lowest values observed in *var. baraquiniana* (Pf023–4.36%) and the highest in *var. ellisonii* (Pf064–38%). The SIRE lineage also exhibited high variation among accessions, more than 10-fold, reaching up to 10.79% in *var. nigelliflora* (Pf007). Other repeat lineages were less abundant and contributed less to overall repeat fraction (Table S5).

Satellite DNAs also exhibited marked variation in abundance among populations, with the lowest values observed in *var. foetida* (Pf031–3.17%) and *var. ellisonii* (Pf153–3.89%), whereas the highest value was detected in *var. baraquiniana* (Pf008–10.65%; Table 3). Variation in ribosomal DNA content was less pronounced, with the 35S rDNA most abundant in *var. baraquiniana* (Pf023–8.34%) and least abundant in *var. nigelliflora* (Pf007–1.27%). The 5S rDNA fraction was generally below 1% across all accessions (Table S5).

Except for var. *acapulsensis*, whose samples formed a monophyletic group and showed similar abundance profiles across the different repeat classes, the remaining varieties were not monophyletic. Relationships among accessions follow a predominantly geographic pattern based on both plastidial and nuclear DNA data (Figs. 6, S6 and S7). The variation observed within each variety was also evident when accessions were grouped into the four major clades, suggesting that factors beyond phylogenetic relationships contribute to shaping repeat abundance.

Although most clusters were shared across all accessions, the largest differences in the abundance of individual clusters involved satDNA and rDNA. The most divergent accessions were Pf008, Pf023, and Pf057, which belonged to three different clades and two distinct varieties (Figs. 1, 6). Analysis of satDNA abundance indicated that the largest variation occurred in PfoSat01-27 (ranging from 2.06% to 9.75%) and PfoSat02-31 (0.11% to 3.97%), corresponding to differences of approximately 4.7-fold and 36-fold, respectively (Table 3).

Table 3
Proportional abundance (%) of the main satellite DNAs identified in the comparative analysis among individuals of different *Passiflora foetida* varieties

Satellites	**PfoSat01-27**	**PfoSat02-31**	**PquSat01-100**	**PquSat06-1083**	**PorSat04-1800**
var. *acapulsensis*					
PF071	4.44%	0.15%	0.24%	0.05%	0.09%
PF078	5.56%	0.52%	0.49%	0.03%	0.03%
PF102	4.73%	0.13%	0.43%	0.04%	0.11%
*v*ar. *baraquiniana*					
PF008	9,75%	0.54%	0.33%	0.01%	0.01%
PF018	3.80%	0.31%	0.32%	0.04%	0.14%
PF023	3,42%	3.97%	0.77%		0.01%
*v*ar. *ellisonii*					
PF001	2.84%	0.50%	0.42%	0.02%	0.08%
PF064	3.15%	0.92%	0.57%	0.02%	0.03%
PF153	2.75%	0.55%	0.50%	0.01%	0.08%
*v*ar. *foetida*					
PF031	2.66%	0.11%	0.28%	0.02%	0.09%
PF057	2.06%	0.15%	0.12%	0.02%	0.03%
PF107	4.89%	0.26%	0.39%	0.03%	0.11%
*v*ar. *nigelliflora*					
PF007	6.10%	0.10%	0.13%	0.05%	0.09%
PF020	5.33%	0.21%	0.23%	0.02%	0.11%
PF085	4.64%	0.23%	0.17%	0.03%	0.06%

3.4 Comparative analysis among species of section *Dysosmia*

The composition of the repetitive genome fraction in three species of *Passiflora* section *Dysosmia* (*P. ciliata*, *P. foetida*, and *P. vesicaria*) revealed a degree of variation comparable to the variation observed within *P. foetida*. Again, the greatest absolute variation was observed in the abundance of the Angela lineage, which, although predominant in all three species, accounted for 17.41% in *P. ciliata*, 22.41% in *P. foetida*, and 28.66% in *P. vesicaria*. In contrast, SIRE lineage exhibited the highest relative variation, from 2.85% in *P. ciliata*, to 10.17% in *P. vesicaria* (Table S6; Figs. S8 and S9). The largest divergence of *P. ciliata* was clearly observed in the analysis of individual repeat clusters, which did not align with the phylogenetic inference based on plastomes (Figure S8). This pattern was reinforced by the abundances of five satDNA families, one of which was specific to *P. ciliata*, while the others were shared among species, including the potentially centromeric satellite PfoSat01-27. The

greatest satDNA divergence was observed in *P. ciliata*, which showed a larger proportion of PclSat01-697 (0.84%) and PfoSat01-27 (2.95%; Table 2).

4. DISCUSSION

4.1 *Passiflora foetida* and the subgenus *Passiflora*

The phylogenetic inference presented here corroborated *P. foetida* and section *Dysosmia* as sister to the remaining sections of the subgenus *Passiflora* (Cauz-Santos et al., 2020; Pacheco et al., 2020; Sader et al., 2021), as well as the positions of *P. ligularis* and *P. incarnata*. However, the position of *P. coccinea* diverged from earlier results (Figure S1), which may be related to the use of a larger dataset in the present analysis, despite the lower species sampling.

In *P. foetida*, the Ty1/copia superfamily showed high abundance (29%), consistent with the pattern observed in most species of the subgenus *Passiflora* (Pamponét et al., 2019). This superfamily is mainly represented by the Angela and SIRE lineages, corroborating previous genome-based characterization (Zou et al., 2023). The predominance of Ty1/copia was also observed in *P. coccinea* and *P. cincinnata*, whereas the other analysed species exhibited a higher proportion of Ty3/gypsy elements. The Ty1/copia Angela and Ty3/gypsy Tekay lineages have been confirmed as the main contributors to genome size expansion in the genus, particularly within the subgenus *Passiflora* (Pamponét et al., 2019; Sader et al., 2021).

Passiflora foetida exhibited a very low abundance of Ty3/gypsy elements, especially Tekay (1.37%), which is likely associated with the small genome size of this species (Yokoto, 2011). Considering the higher proportion of Tekay elements in other genomes, including *P. organensis* (Sader et al., 2021), and the phylogenetic position of *P. foetida*, our data may suggest either a lineage-specific elimination of Tekay in *P. foetida* (Ibarra-Laclette et al., 2013) or an independent amplification of this element in the subgenera *Passiflora* and *Decaloba*.

4.2 Variation within *P. foetida*

The phylogenetic relationships among the *P. foetida* accessions sampled here were consistent with those reported by Hopley et al. (2021), who observed a predominant geographic pattern. The assessment of the repeatome in *P. foetida* at the intraspecific level, however, did not reflect its phylogenetic/geographic relationships. Nevertheless, its repeatome was highly heterogeneous (24.58%–64.10%), comparable to that observed among species of the genus (16.79%–78.56%), which encompasses more than a tenfold variation in DNA content (Sader et al., 2021). Variation in the abundance of the repetitive fraction is generally associated with variation in genome size in plant species (Albach & Greilhuber, 2004; Novák et al., 2020). However, the current literature shows no evidence of genome size differences among *P. foetida* accessions or species complex (Yokoto et al., 2011; Leite et al., 2019; Mikovski et al., 2021; Bugallo et al., 2023; Zou et al., 2023; Zirpoli et al., 2025), what need further investigation.

Moreover, the repeatome of *P. foetida* is particularly diverse when compared to other species of the subgenus, suggesting a dynamic turnover in this species. Although the data corroborate the individual characterization, where individuals showed high abundance of Ty1/copia and scarcity of Ty3/gypsy, in two accessions (PF008 and PF023), for example, the proportion of tandem repeats exceeds that of Ty1/copia. Literature data show that different species and even distinct populations of the same species may develop unique profiles of repetitive elements or variable patterns of sequences due to mutations and genomic rearrangements over time (Oliver et al., 2013; Ricc et al., 2018). This has been recently demonstrated, especially in pangenomic studies of species such as *Arabidopsis thaliana* L. (Kang et al., 2023; Lian et al., 2024) and *Solanum tuberosum* L. (Cheng et al., 2025). Divergence in the proportions of the repetitive fractions among *P. foetida* accessions, caused by fluctuations (amplification/deletion) of these elements, may be associated with environmental pressures or other factors yet to be investigated (Pons & Gillespie, 2014; Feiner et al., 2016; Castro et al., 2024).

Phylogenetic analyses of the plastidial and nuclear datasets, together with repeatome characterization, did not support the subdivision of *P. foetida* into the currently accepted varieties. Nevertheless, the extensive intraspecific variation observed may be associated with reproductive isolation among accessions, impacting chromosomal pairing during meiosis or resulting in other incompatibilities (Levy et al., 2013; Garrido-Ramos et al., 2015; Castro et al., 2024). Recent studies indicate that repetitive DNA transposition may be influenced by the environment, often leading to the activation or silencing of genes (Kanazawa et al., 2009; Canapa et al., 2020; Castro et al., 2024). The different lineages of *P. foetida* require further characterization using an integrative approach, given that the morphological characters used by Vanderplanck (2013) to define varieties were shown to be homoplastic.

4.3 *Dysosmia* Section

The phylogeny of section *Dysosmia* positioned *P. foetida* as sister to the remaining two species (*P. vesicaria* and *P. ciliata*), differing from the topology reported by Hopley et al. (2021), who investigated the same accessions under *P. foetida sensu lato*. Both topologies are inconsistent with the greater divergence observed in the *P. ciliata* repeatome, especially in its satellitome, suggesting that the phylogenetic relationships and

taxonomic status of species within this section should be re-evaluated (Vanderplank, 2013; Parteka et al., 2021 Svoboda, 2023). Despite the greater similarity between the clusters of *P. foetida* and *P. vesicaria* compared to those of *P. ciliata*, the differences in repetitive DNA abundance among these species are smaller than those observed among the varieties of *P. foetida*.

4.4 The Satellitome of *P. foetida*

Only three satDNA were identified by TAREAN in the short-read analysis, none of which similar to previously described *Passiflora* satDNAs. These sequences were amplified exclusively in *P. foetida* and closely related species within the section *Dysosmia*. Among them, only PfoSat01-27 was detected in the broader comparative analysis, confirming its specificity to *P. foetida sensu lato*. In addition to the similarity with previously described satellites in the genus, the use of the *Passiflora* repeat database revealed low similarity between the 35S rDNA sequence and a new satDNA (PfoSat02-31). The same had been previously observed for PquSat01-100, from *P. quadrangularis*, suggesting multiple origins for satDNA in the genus from the 35S rDNA (Sader et al., 2021). The variability of 5S rDNA observed in this study has been previously reported in the group, with most accessions exhibiting a single chromosomal pair of sites (Zirpoli et al., 2024). And the heteromorphism in 5S rDNA sites has been documented among cultivars of *P. edulis* (Marróquín et al., 2023).

Satellite DNA typically forms blocks in the heterochromatic regions of chromosomes (Heslop-Harrison & Schwarzacher, 2011; Ribeiro et al., 2017). Satellite repeats may occur in subtelomeric or interstitial regions but are most found in centromeres (Garrido-Ramos, 2015). The section-specific satDNA PfoSat01-27 hybridized to the centromeric region of nine chromosome pairs of *P. foetida* and was detected *in silico*, supporting our cytogenetic results. Considering all satDNA localized so far in *Passiflora*, none had been typically centromeric (Costa et al., 2021; Sader et al., 2021). Although its association with centromeric proteins remains to be demonstrated, its chromosomal distribution suggests that PfoSat01-27 is a centromeric sequence. As a putative centromeric satDNA, variability at the interspecific level is not uncommon (Macas et al., 2010; Melters et al., 2013; Zhang et al., 2013; Garrido-Ramos et al., 2015). But the fact that it is section-specific and that its abundance varies widely among chromosomes of the species, even between homologous chromosomes generating heteromorphic pairs, suggests that this centromeric repeat is a recent evolutionary acquisition in the genus.

5. CONCLUSION

Our results highlight the important role played by the repetitive fraction in the genome evolution of *P. foetida*, revealing patterns of high intra- and interspecific variation. The presence of satellite sequences shared with species from other subgenera supports its phylogenetic position; however, the intraspecific diversity of its repeatome, as well as the inconsistencies with phylogenetic and taxonomic data, reinforce the uncertain relationships among *P. foetida* varieties and closely related species. Finally, the identification of a potential centromeric satellite in *P. foetida* and related species suggests a recent evolutionary acquisition within section *Dysosmia*.

Declarations

Funding

This work was supported by the Fundação de Amparo a Ciência e Tecnologia do Estado de Pernambuco (FACEPE) for a scholarship to AM, the Conselho Nacional de Desenvolvimento Científico e Tecnológico (CNPq, Brazil) for the research fellowship to APH (312694/2021–0) and previous scholarship to AM, also supported by PROPESQI/UFPE. This research was in part supported by CAPES (Coordenação de Aperfeiçoamento de Pessoal de Nível Superior, Finance Code 001).

Author Contribution

AM performed bioinformatic and cytogenetic analyses and drafted the manuscript. JN and MAS labelled FISH probes, analysed the data and assisted with manuscript writing. GL performed phylogenetic analyses and contributed to manuscript writing. DCI provided plant material and taxonomic identification. APH designed the experiments, analysed the data, and assisted with manuscript writing. All authors have read and agreed to the published version of the manuscript.

Acknowledgement

We thank Prof. Dr. Marcelo Guerra (UFPE), Dr. Nilton Tadeu V. Junqueira (Embrapa Cerrados) and Dr. Onildo Nunes de Jesus (Embrapa Mandioca e Fruticultura) for providing P. foetida seeds. We are grateful to the ELIXIR-CZ Research Infrastructure Project (LM2015047) for providing computational resources for RepeatExplorer analysis.

Data Availability

All data generated or analysed during this study are available in GenBank (listed in the manuscript or in Supplementary Tables) or included in the manuscript.

References

1. Albach DC, Greilhuber J (2004) Genome size variation and evolution in *Veronica*. *Annals of Botany* 94(6):897–911. https://doi.org/10.1093/aob/mch219
2. Bernacci LC, Nunes TS, Mezzonato AC, Milward-de-Azevedo MA, Imig DC, Cervi AC (in memoriam) (2025) *Passiflora in Flora e Funga do Brasil*. Jardim Botânico do Rio de Janeiro.
3. Bugallo VL, Facciuto GR, Poggio L (2023) Genome size in Argentinean species of *Passiflora* genus: cytological and phenotypical correlates. *Rodriguésia* 74:e00872022. https://doi.org/10.1590/2175-7860202374046
4. Canapa A, Biscotti MA, Barucca M, Carducci F, Carotti E, Olmo E (2020) Shedding light upon the complex net of genome size, genome composition and environment in chordates. *The European Zoological Journal* 87(1):192–202. https://doi.org/10.1080/24750263.2020.1747558
5. Carareto CMA, Monteiro-Vitorello CB, Van Sluys MA (eds) (2015) *Elementos de transposição: diversidade, evolução, aplicações e impacto nos genomas dos seres vivos*. SciELO-Editora FIOCRUZ.
6. Castro N, Vilela B, Mata-Sucre Y, Marques A, Gagnon E, Lewis GP, … Souza G (2024) Repeatome evolution across space and time: Unravelling repeats dynamics in the plant genus *Erythrostemon* Klotzsch (Leguminosae Juss). *Molecular Ecology* e17510. https://doi.org/10.1111/mec.17510
7. Cauz-Santos LA, da Costa ZP, Callot C, Cauet S, Zucchi MI, Bergès H, … Vieira MLC (2020) A repertory of rearrangements and the loss of an inverted repeat region in *Passiflora* chloroplast genomes. *Genome Biology and Evolution* 12(10):1841–1857. https://doi.org/10.1093/gbe/evaa155
8. Cauz-Santos LA, da Costa ZP, Sader MA, van den Berg C, Vieira MLC (2025) Chloroplast genomic insights into adaptive evolution and rapid radiation in the genus *Passiflora* (Passifloraceae). *BMC Plant Biology* 25(1):192. https://doi.org/10.1186/s12870-025-06210-9
9. Cheng L, Wang N, Bao Z, et al (2025) Aproveitando um pangenoma em fases para o projeto de haplótipos de batata híbrida. *Nature* 640:408–417. https://doi.org/10.1038/s41586-024-08476-9
10. Cuadrado Á, Golczyk H, Jouve N (2009) A novel, simple and rapid nondenaturing FISH (ND-FISH) technique for the detection of plant telomeres. Potential used and possible target structures detected. *Chromosome Research* 17(6):755–762. https://doi.org/10.1007/s10577-009-9060-z
11. Cuadrado Á, Jouve N (2010) Chromosomal detection of simple sequence repeats (SSRs) using nondenaturing FISH (ND-FISH). *Chromosoma* 119(5):495–503. https://doi.org/10.1007/s00412-010-0273-x. https://doi.org/10.1007/s00412-010-0273-x
12. Drummond AJ, Ho SY, Phillips MJ, Rambaut A. Relaxed phylogenetics and dating with confidence. PLoS biology. 2006;4(5):e88. https://doi.org/10.1371/journal.pbio.0040088
13. Feiner N (2016) Accumulation of transposable elements in Hox gene clusters during adaptive radiation of Anolis lizards. *Proceedings of the Royal Society B: Biological Sciences* 283(1840):20161555. https://doi.org/10.1098/rspb.2016.1555
14. Garrido-Ramos MA (2017) Satellite DNA: an evolving topic. *Genes* 8(9):230. https://doi.org/10.3390/genes8090230
15. Garrido-Ramos MA (2015) Satellite DNA in plants: more than just rubbish. *Cytogenetic and Genome Research* 146(2):153–170. https://doi.org/10.1159/000437008
16. Gordon A, Hannon GJ (2010) FASTX-Toolkit. Ferramentas de pré-processamento de leituras curtas FASTQ/A. Disponível em: http://www.hannonlab.cshl.edu/fastx_toolkit
17. Hansen AK, Gilbert LE, Simpson BB, Downie SR, Cervi AC, Jansen RK (2006) Phylogenetic relationships and chromosome number evolution in *Passiflora*. *Systematic Botany* 31(1):138–150. https://doi.org/10.1600/036364406775971769
18. Heslop-Harrison JS, Schwarzacher T (2011) Organisation of the plant genome in chromosomes. *The Plant Journal* 66(1):18–33. https://doi.org/10.1111/j.1365-313X.2011.04544.x
19. Hopley T, Webber BL, Raghu S, Morin L, Byrne M (2021) Revealing the introduction history and phylogenetic relationships of *Passiflora foetida* sensu lato in Australia. *Frontiers in Plant Science* 12:651805. https://doi.org/10.3389/fpls.2021.651805
20. Hopley T, Webber BL, Raghu S, Morin L, Byrne M (2026) Genetic insights into the invasion success of a non-native weed: the case of stinking passionflower (*Passiflora foetida* sens. lat.) in Australia. *Biological Invasions* 28:3. https://doi.org/10.1007/s10530-025-03714-1
21. Hua-Van A, Le Rouzic A, Boutin TS, Filée J, Capy P (2011) The struggle for life of the genome's selfish architects. *Biology Direct* 6(1):19. https://doi.org/10.1186/1745-6150-6-19
22. Ibarra-Laclette E, Lyons E, Hernández-Guzmán G, Pérez-Torres CA, Carretero-Paulet L, Chang TH, … Herrera-Estrella L (2013) Architecture and evolution of a minute plant genome. *Nature* 498(7452):94–98. https://doi.org/10.1038/nature12132

23. Kanazawa A, Liu B, Kong F, Arase S, Abe J (2009) Adaptive evolution involving gene duplication and insertion of a novel Ty1/copia-like retrotransposon in soybean. *Journal of Molecular Evolution* 69(2):164–175. https://doi.org/10.1007/s00239-009-9262-1
24. Kang M, Wu H, Liu H, et al (2023) The pan-genome and local adaptation of *Arabidopsis thaliana*. *Nature Communications* 14:6259. https://doi.org/10.1038/s41467-023-42029-4
25. Katoh K, Standley DM (2013) MAFFT multiple sequence alignment software version 7: improvements in performance and usability. *Molecular Biology and Evolution* 30(4):772–780. https://doi.org/10.1093/molbev/mst010
26. Kearse M, Moir R, Wilson A, Stones-Havas S, Cheung M, Sturrock S, … Drummond A (2012) Geneious Basic: an integrated and extendable desktop software platform for the organization and analysis of sequence data. *Bioinformatics* 28(12):1647–1649. https://doi.org/10.1093/bioinformatics/bts199
27. Krosnick SE, Porter-Utley KE, MacDougal JM, Jørgensen PM, McDade LA (2013) New insights into the evolution of *Passiflora* subgenus *Decaloba* (Passifloraceae): phylogenetic relationships and morphological synapomorphies. *Systematic Botany* 38(3):692–713. https://doi.org/10.1600/036364413X670359
28. Leite CT, Ferreira DAT, Vieira AT, Praça-Fontes MM, Ferreira A, Carvalho CR, Clarindo WR (2019) In vitro responses in *Passiflora* species with different chromosome numbers, ploidy levels and nuclear 2C values: revisiting and providing new insights. *Plant Cell, Tissue and Organ Culture* 136(3):549–560. https://doi.org/10.1007/s11240-018-01536-9
29. Levy AA (2013) Transposons in plant speciation. In: *Plant transposons and genome dynamics in evolution*, pp 165–179. DOI:10.1002/9781118500156
30. Lian Q, Huettel B, Walkemeier B, et al (2024) A pan-genome of 69 *Arabidopsis thaliana* accessions reveals a conserved genome structure throughout the global species range. *Nature Genetics* 56:982–991. https://doi.org/10.1038/s41588-024-01715-9
31. Ma D, Dong S, Zhang S, Wei X, Xie Q, Ding Q, … Zhang X (2021) Chromosome-level reference genome assembly provides insights into aroma biosynthesis in passion fruit (*Passiflora edulis*). *Molecular Ecology Resources* 21(3):955–968. https://doi.org/10.1111/1755-0998.13310
32. Macas J, Neumann P, Novák P, Jiang J (2010) Global sequence characterization of rice centromeric satellite based on oligomer frequency analysis in large-scale sequencing data. *Bioinformatics* 26(17):2101–2108. https://cientifica.dracena.unesp.br/index.php/cientifica/article/view/1372
33. Mai DH. Über neue Früchte und Samen aus dem deutschen Tertiär. Paläontologische Zeitschrift. 1960;34(1):73–90. https://doi.org/10.1007/BF02987044
34. Marroquín JAM, Souza MM, Silva GS, Melo CAF, de Oliveira Souza V, Santos-Sanchês RD (2023) Citogenética comparativa em nove cultivares de maracujazeiro azedo (*Passiflora edulis* Sims). *Científica* 51:15. https://cientifica.dracena.unesp.br/index.php/cientifica/article/view/1372
35. Mehrotra S, Goyal V (2014) Repetitive sequences in plant nuclear DNA: types, distribution, evolution and function. *Genomics, Proteomics & Bioinformatics* 12(4):164–171. https://doi.org/10.1016/j.gpb.2014.07.003
36. Melters DP, Bradnam KR, Young HA, Telis N, May MR, Ruby JG, … Chan SW (2013) Comparative analysis of tandem repeats from hundreds of species reveals unique insights into centromere evolution. *Genome Biology* 14(1):R10. https://doi.org/10.1186/gb-2013-14-1-r10
37. Melo NFD, Guerra M (2021) The karyotype of *Adenia* and the origin of the base number x = 12 in Passifloroideae (Passifloraceae). *Anais da Academia Brasileira de Ciências* 93:e20201852. https://doi.org/10.1590/0001-3765202120201852
38. Neumann P, Novák P, Hoštáková N, Macas J (2019) Systematic survey of plant LTR-retrotransposons elucidates phylogenetic relationships of their polyprotein domains and provides a reference for element classification. *Mobile DNA* 10:1. https://doi.org/10.1186/s13100-018-0144-1
39. Novák P, Neumann P, Macas J (2020) Global analysis of repetitive DNA from unassembled sequence reads using RepeatExplorer2. *Nature Protocols* 15(11):3745–3776. https://doi.org/10.1038/s41596-020-0400-y
40. Oliver KR, McComb JA, Greene WK (2013) Transposable elements: powerful contributors to angiosperm evolution and diversity. *Genome Biology and Evolution* 5(10):1886–1901. https://doi.org/10.1093/gbe/evt141
41. Pacheco TG, Lopes ADS, Welter JF, Yotoko KSC, Otoni WC, Vieira LDN, … Rogalski M (2020) Plastome sequences of the subgenus *Passiflora* reveal highly divergent genes and specific evolutionary features. *Plant Molecular Biology* 104(1):21–37. https://doi.org/10.1007/s11103-020-01020-z
42. Pamponét VCC, Souza MM, Silva GS, Micheli F, de Melo CAF, de Oliveira SG, … Corrêa RX (2019) Low coverage sequencing for repetitive DNA analysis in *Passiflora edulis* Sims: citogenomic characterization of transposable elements and satellite DNA. *BMC Genomics* 20:262. https://doi.org/10.1186/s12864-019-5576-6
43. Parteka LM, De Mattos L, Richardo J, Fagundes BS, Silverio A (2021) *Passiflora coelestis*, a new species of *Passiflora* section Dysosmia (Passifloraceae sensu stricto) from Southern Brazil. *Phytotaxa* 516(2):140–158. https://doi.org/10.11646/phytotaxa.516.2.2

44. Pedrosa-Harand A, de Almeida CCS, Mosiolek M, Blair MW, Schweizer D, Guerra M (2006) Extensive ribosomal DNA amplification during Andean common bean (*Phaseolus vulgaris* L.) evolution. *Theoretical and Applied Genetics* 112(5):924–933. https://doi.org/10.1007/s00122-005-0196-8
45. Pons J, Gillespie RG (2004) Evolution of satellite DNAs in a radiation of endemic Hawaiian spiders: does concerted evolution of highly repetitive sequences reflect evolutionary history? *Journal of Molecular Evolution* 59(5):632–641. https://doi.org/10.1007/s00239-004-2655-2
46. Price MN, Dehal PS, Arkin AP (2009) FastTree: computing large minimum evolution trees with profiles instead of a distance matrix. *Molecular Biology and Evolution* 26(7):1641–1650. https://doi.org/10.1093/molbev/msp077
47. Rambaut A, Drummond AJ, Xie D, Baele G, Suchard MA. Posterior summarization in Bayesian phylogenetics using Tracer 1.7. Systematic biology. 2018;67(5):901–4. https://doi.org/10.1093/sysbio/syy032
48. Ribeiro T, Marques A, Novák P, Schubert V, Vanzela AL, Macas J, … Pedrosa-Harand A (2017a) Centromeric and non-centromeric satellite DNA organisation differs in holocentric *Rhynchospora* species. *Chromosoma* 126(2):325–335. https://doi.org/10.1007/s00412-016-0616-3
49. Ribeiro T, Dos Santos KG, Richard MM, Sévignac M, Thareau V, Geffroy V, Pedrosa-Harand A (2017b) Evolutionary dynamics of satellite DNA repeats from *Phaseolus* beans. *Protoplasma* 254(2):791–801. https://doi.org/10.1007/s00709-016-0993-8
50. Ricci M, Peona V, Guichard E, Taccioli C, Boattini A (2018) Transposable elements activity is positively related to rate of speciation in mammals. *Journal of Molecular Evolution* 86(5):303–310. https://doi.org/10.1007/s00239-018-9847-7
51. Ruiz-Ruano FJ, López-León MD, Cabrero J, Camacho JPM (2016) High-throughput analysis of the satellitome illuminates satellite DNA evolution. *Scientific Reports* 6:28333. https://doi.org/10.1038/srep28333
52. Sader M, Vaio M, Cauz-Santos LA, Dornelas MC, Vieira MLC, Melo N, Pedrosa-Harand A (2021) Large vs small genomes in *Passiflora*: the influence of the mobilome and the satellitome. *Planta* 253(4):86. https://doi.org/10.1007/s00425-021-03598-0
53. Sader MA, Dias Y, Costa ZPD, Munhoz C, Penha H, Bergès H, … Pedrosa-Harand A (2019) Identification of passion fruit (*Passiflora edulis*) chromosomes using BAC-FISH. *Chromosome Research* 27(4):299–311. https://doi.org/10.1007/s10577-019-09614-0
54. Suchard MA, Lemey P, Baele G, Ayres DL, Drummond AJ & Rambaut A (2018) Bayesian phylogenetic and phylodynamic data integration using BEAST 1.10 *Virus Evolution* 4, vey016. DOI:10.1093/ve/vey016
55. Svoboda HT (2023) Five new combinations in *Passiflora* sect. Dysosmia (Passifloraceae). *Novon: A Journal for Botanical Nomenclature* 31(1):163–168. https://doi.org/10.3417/2023841
56. Svoboda HT, Macdougal JM, Ballard Jr HE (2016) Typifications and nomenclatural notes in *Passiflora* section Dysosmia (Passifloraceae). *Phytotaxa* 288(2):101. DOI: 10.11646/phytotaxa.288.2.1
57. Ulmer T, MacDougal JM (2004) *Passiflora: passionflowers of the world*. Timber Press, OR.
58. Vanderplank J (2013) A revision of *Passiflora* section Dysosmia: Passifloraceae. *Curtis's Botanical Magazine* 30(4):318–387. https://doi.org/10.1111/curt.12050
59. Waminal NE, Pellerin RJ, Kim NS, Jayakodi M, Park JY, Yang TJ, Kim HH (2018) Rapid and efficient FISH using pre-labeled oligomer probes. *Scientific Reports* 8:8224. https://doi.org/10.1038/s41598-018-26667-z
60. Xia Z, Huang D, Zhang S, Wang W, Ma F, Wu B, … Song S (2021) Chromosome-scale genome assembly provides insights into the evolution and flavor synthesis of passion fruit (*Passiflora edulis Sims*). *Horticulture Research* 8. https://doi.org/10.1038/s41438-020-00455-1
61. Yotoko KS, Dornelas MC, Togni PD, Fonseca T C, Salzano FM, Bonatto SL, Freitas LB (2011) Does variation in genome sizes reflect adaptive or neutral processes? New clues from *Passiflora*. *PLoS One* 6(3):e18212. https://doi.org/10.1371/journal.pone.0018212
62. Yu Y, Ouyang Y, Yao W (2018) shinyCircos: an R/Shiny application for interactive creation of Circos plot. *Bioinformatics* 34(7):1229–1231. https://doi.org/10.1093/bioinformatics/btx763
63. Zirpoli, B., Monteiro, A., Rodriguez, P. E., Viana, B. L., Maciel, J. R., Pedrosa-Harand, A., & Sader, M. A. (2025). Two species and two karyotypes? Cytogenetic differentiation between *Passiflora foetida* L. and P. *vesicaria* L. (Passifloraceae). *Systematics and Biodiversity*, 23(1). https://doi.org/10.1080/14772000.2025.2565219
64. Zhang T, Talbert PB, Zhang W, Wu Y, Yang Z, Henikoff JG, … Jiang J (2013) The CentO satellite confers translational and rotational phasing on cenH3 nucleosomes in rice centromeres. *Proceedings of the National Academy of Sciences* 110(50):E4875–E4883. https://doi.org/10.1073/pnas.1319548110
65. Zou Y, Wang J, Peng D, Zhang X, Tembrock LR, Yang J, … Wu Z (2023) Multi-integrated genomic data for *Passiflora foetida* provides insights into genome size evolution and floral development in *Passiflora*. *Molecular Horticulture* 3(1):27. https://doi.org/10.1186/s43897-023-00076-x.

Figures

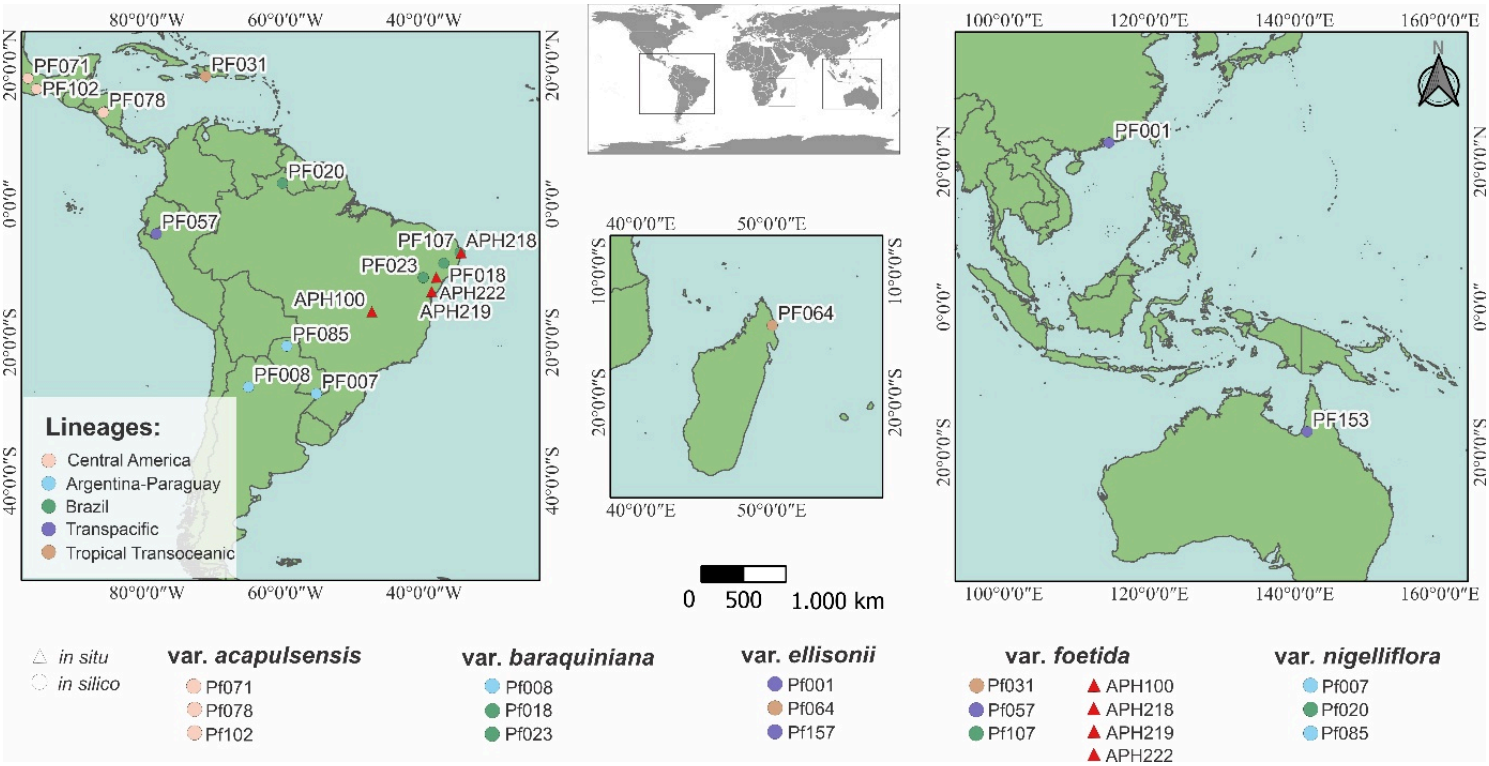

Figure 1

Geographic distribution of the analysed *P. foetida* accessions in relation to their phylogenetic clustering and taxonomic identification. Accessions represented by circles were used for *in silico* analyses, whereas those represented by triangles were used for *in situ* analyses.

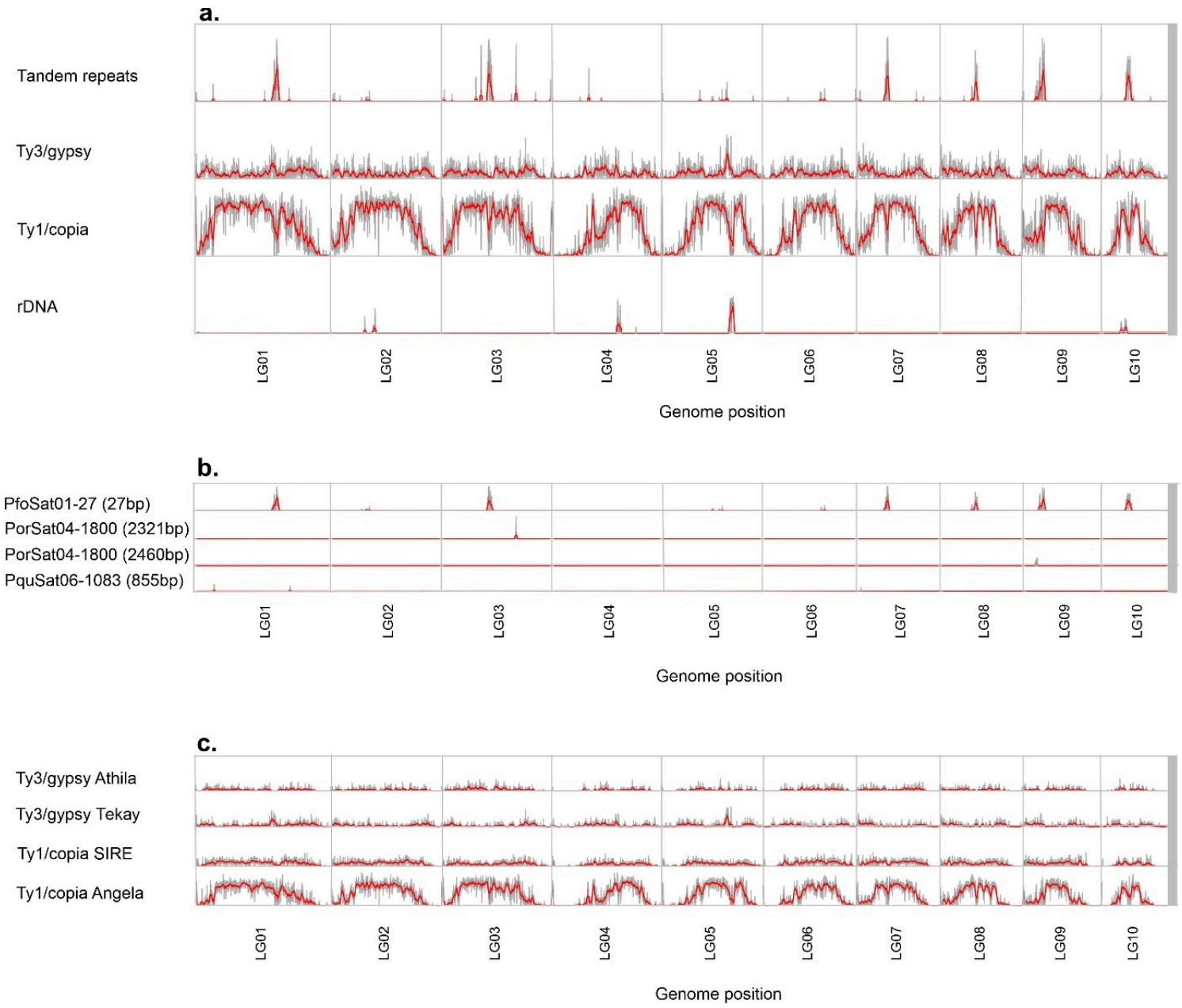

Figure 2

In silico distribution of repeats in *P. foetida* genome. a. overall distribution of the main repetitive DNA fractions in the genome. b. Main tandem repeats. c. Main LTR-RT lineages.

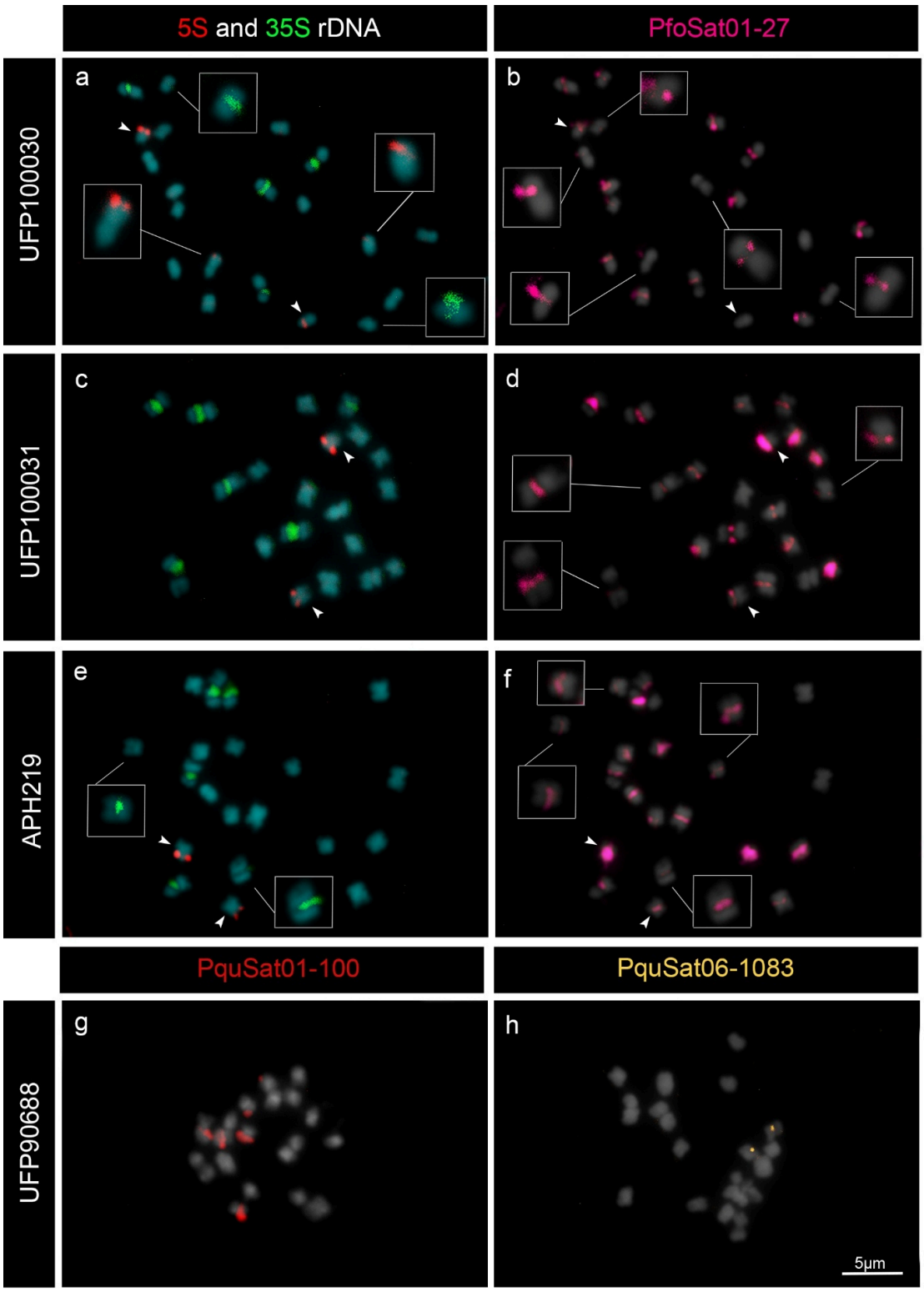

Figure 3

In situ localization of tandem repeats in *Passiflora foetida* metaphase chromosomes. 5S rDNA (red) and 35S rDNA (green) in a, c, e. Species-specific satellite PfoSat01-27 (pink) in different *P. foetida*accessions in b, d, f. PquSat01-100 (red) in g. PquSat06-1083 (yellow) in h. Insets show weaker signals in higher brightness. Arrowheads point to heteromorphic chromosome pairs.

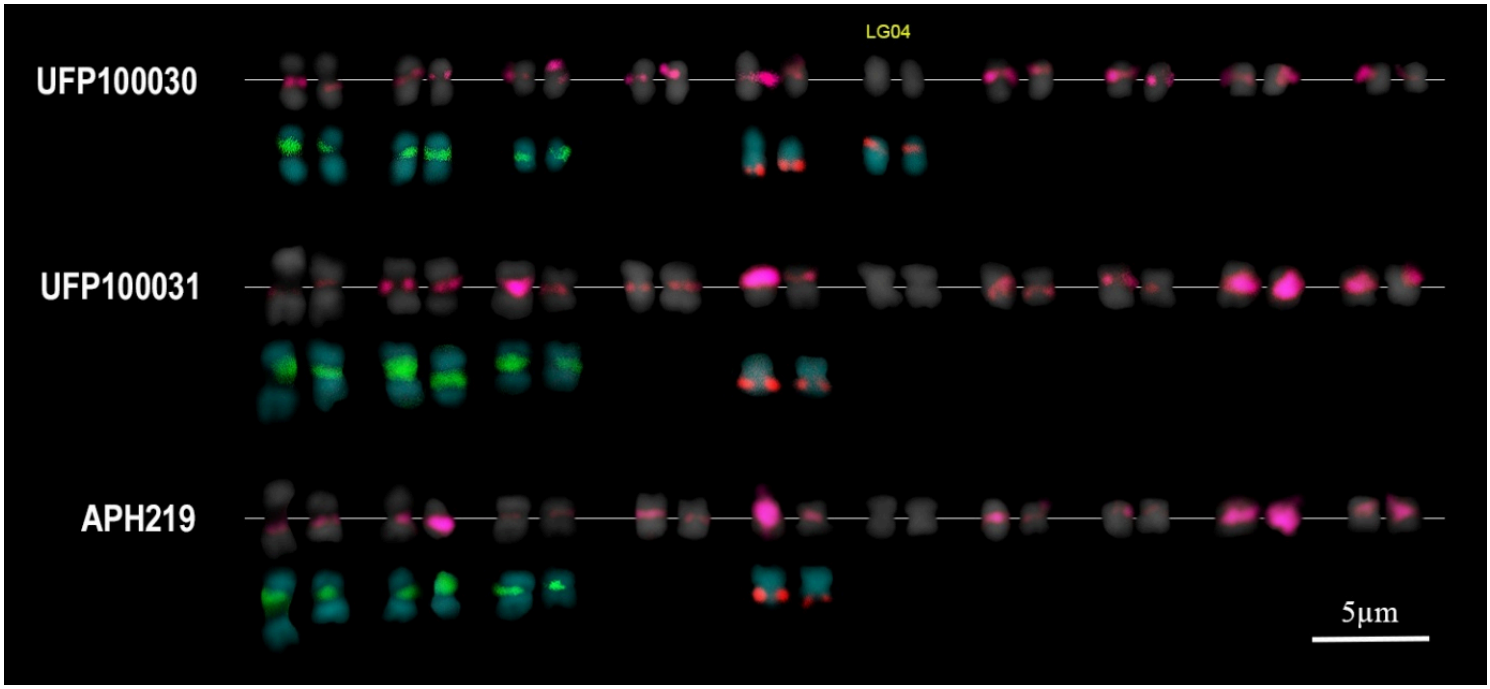

Figure 4

Karyogram showing the chromosomal distribution of the most abundant satellite of *P. foetida*, PfoSat01-27 (pink), as well as the 35S (green) and 5S (red) rDNA. Heteromorphisms between homologous chromosomes in the abundance of satDNA signals cold be detected using rDNA to identify some chromosome pairs. The chromosome pair with lower abundance of PfoSat1-27 was tentatively identified as pseudochromosome 4 (LG04), while the pair with 5S rDNA as LG03 based on the *in silico* distribution of this repeat (Figure S3).

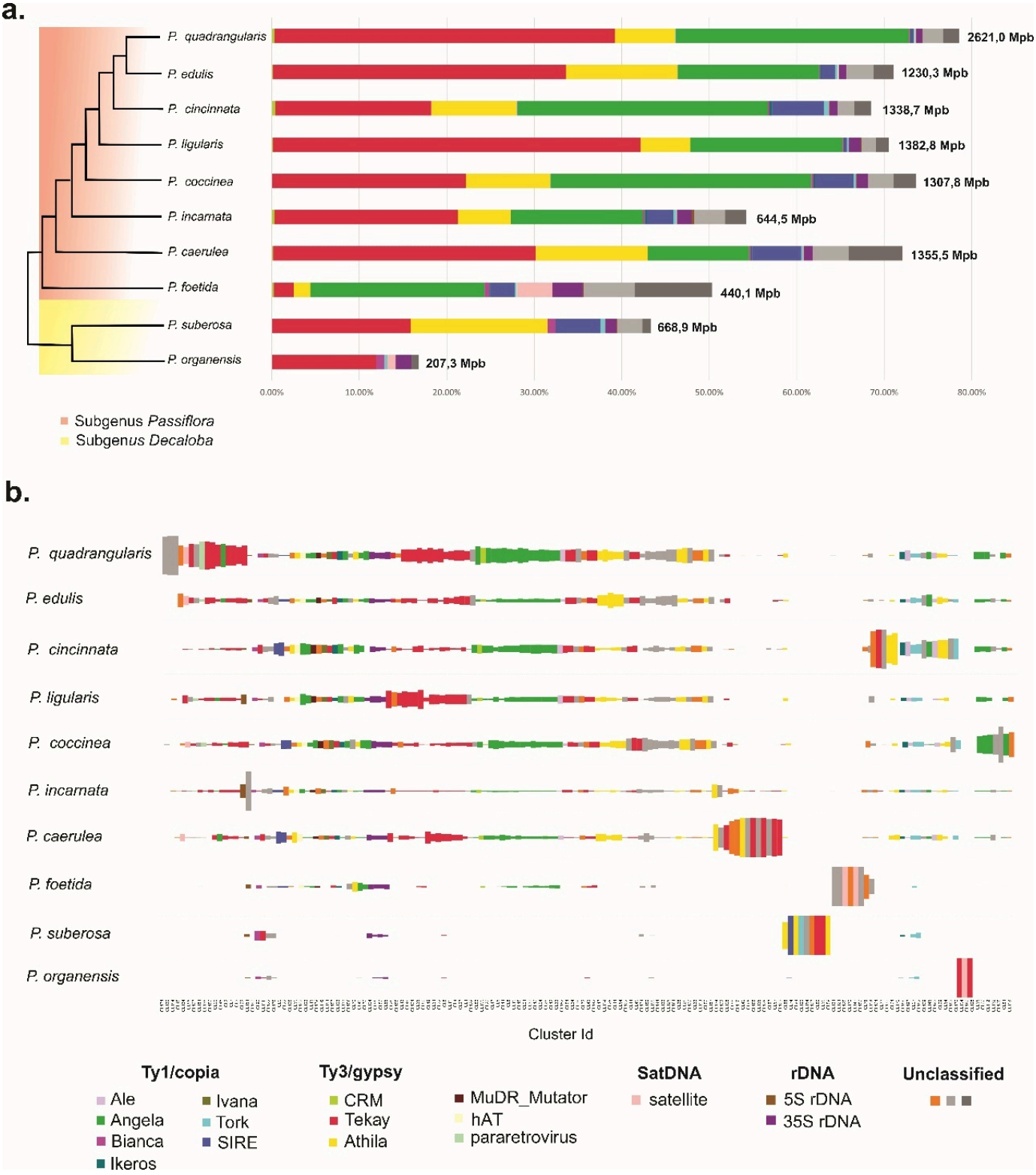

Figure 5

Comparative analysis of repetitive DNA in *Passiflora* genomes of the subgenera *Passiflora*and *Decaloba* (outgroup) represented according to their phylogenetic relationships inferred from plastome assemblies using *P. edulis* as reference. **a.** Abundances per repeat class and lineage as percentage of the total genome size; **b.** Abundances per cluster proportional to the sizes of the bars. Annotations indicated by colours**.**

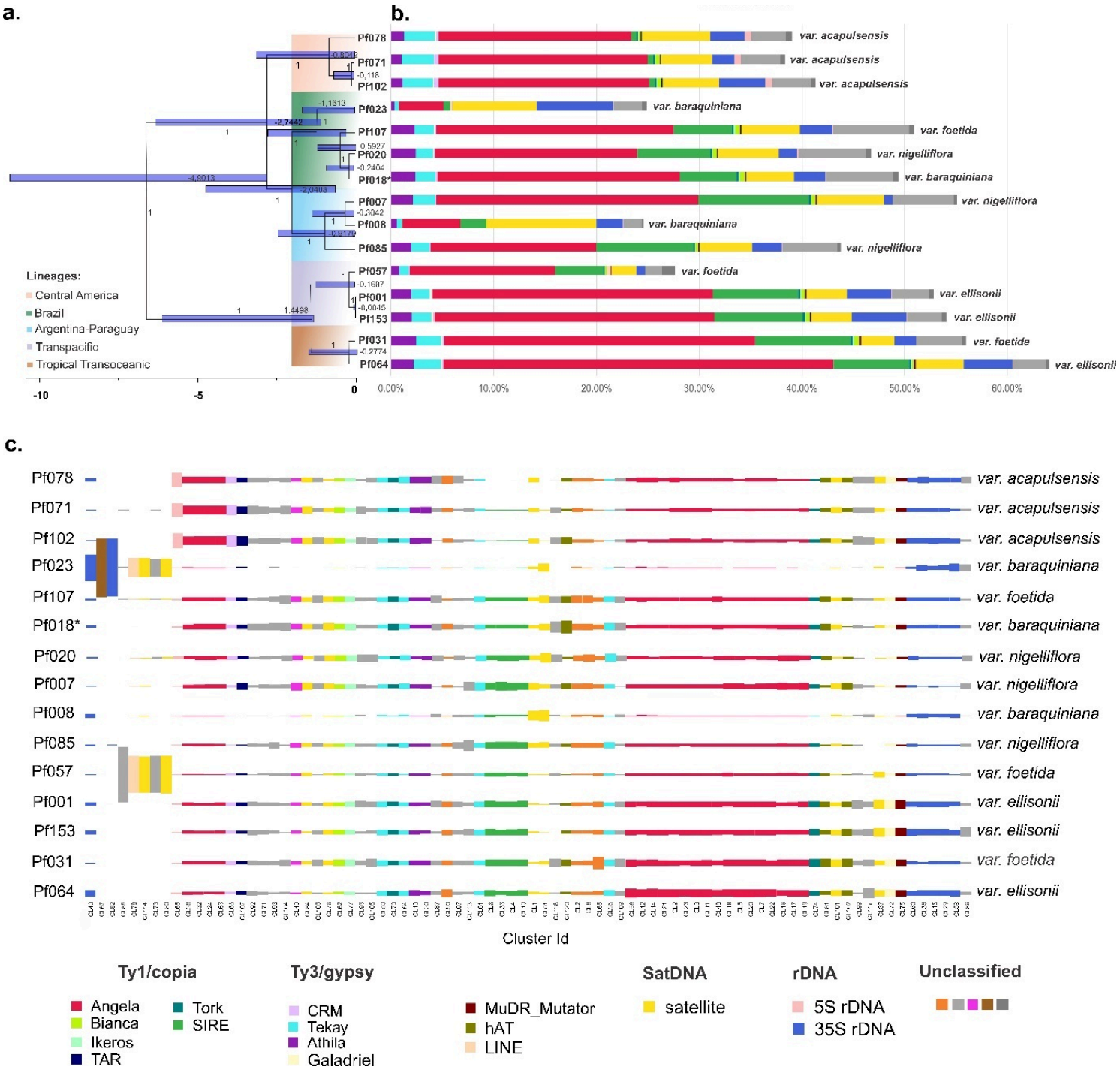

Figure 6

Comparative analysis of repetitive DNA abundance across different *P. foetida*accessions representing distinct varieties. **a.** Phylogenetic relationships with divergence time estimates inferred from plastome assemblies; **b.** Abundances per repeat class and lineage as percentage of the total genome size; **b.** Abundances per cluster proportional to the sizes of the bars. Annotations indicated by colours.

Supplementary Files

This is a list of supplementary files associated with this preprint. Click to download.

- SupplementaryMaterial.docx